Experimental Thermal and Fluid Science 55 (2014) 128–139

Contents lists available at ScienceDirect

Experimental Thermal and Fluid Science

journal homepage: www.elsevier.com/locate/etfs

Horizontal turbulent channel flow interacted by a single large bubble

Yoshihiko Oishi *, Yuichi Murai

Laboratory for Flow Control, Division of Energy and Environmental Systems, Faculty of Engineering, Hokkaido University, Kita-13 Nishi-8 Kita-ku, Sapporo 060-8628, Japan

ARTICLE INFO

Article history:
Received 5 January 2014
Received in revised form 18 February 2014
Accepted 19 February 2014
Available online 12 March 2014

Keywords:
Bubble
Horizontal channel flow
Turbulent flow
PTV
Drag reduction

ABSTRACT

Flow field modified by a single large bubble in a horizontal wall turbulent boundary layer is measured by particle tracking velocimetry. We focus on intermediate bubble size being comparable to the thickness of boundary layer to find out the events altering the original turbulent shear stress field. The results are all presented by quantities relative to single phase flow on Lagrangian grid system that moves with the bubble. The measurement results reveal bubble-produced secondary flow around itself, which involves twin roll vortices, separation on the bubble surface, and strong sweeping flow. For a small and nearly spherical bubble, the sweeping flow is provided strongly to enhance the turbulent momentum exchange while negative exchange is detected for a large flat bubble. This effective length approximately corresponds to the size of the bubble.

1. Introduction

Reducing skin friction drag has long been an important issue in fluids engineering. To achieve this goal, the use of bubbles is recognized as one of the feasible techniques for large facilities such as ships and pipelines [1]. This is because of the fact that bubbles can be generated from the atmosphere around the target system, and air bubbles do not damage the circumferential system environment. Air bubble drag-reduction mechanisms are generally classified into two regimes [2]. One is the so-called microbubble method, which utilizes the change that occurs in the turbulent flow properties upon mixing in small spherical bubbles. The first experiment to confirm this effect was reported by McCormick and Bhttacharyya [3], who employed electrolysis to generate microbubbles in water to estimate the reduction in drag of a submerged hull. After this finding, a number of experiments were carried out to elucidate the physical mechanism and to examine the applicability to different targets [4–9]. Building on these works, Madavan et al. [4] and Sanders et al. [10] showed that the buoyancy of microbubbles significantly helps raise the persistency of drag reduction for the flat-plate boundary layer. Huang et al. [11] and Hara et al. [12] studied how the mixing of bubbles/microbubbles promotes and suppresses the transition to turbulence in a transitional regime of a horizontal channel. In a more physics-oriented study, Taylor–Couette flow was used to discover which flow mode best suits the bubbles mixed into the flow to reduce drag [13,14].

The second drag-reduction mechanism, called the air-film method, uses an air-film to separate a solid wall and high-speed liquid flow [15,16]. This drag-reduction mechanism is relatively simple, but maintaining an air-film for a long time above the high-shearing liquid flow presents a serious problem. The Kelvin–Helmholtz instability that arises at the gas–liquid interface breaks the gravitational stratification of the two phases and results in the generation of bubbles. Katsui et al. [17] confirmed with a tanker model that, as long as the air-film is maintained, the drag-reduction ratio is proportional to the air-film area occupying the tanker's wall.

For both the microbubble and air-film method, a long-term issue remains of whether the intermediate-sized bubbles (1–10 mm) can reduce drag. Because in water the typical bubble size is usually in this intermediate range, it is important to investigate the functions of intermediate bubbles. For these bubbles, one concern is the effective viscosity as a function of the capillary number [18,19], which expresses the degree of viscous bubble deformation in laminar flow. In turbulent flow, deformation occurs with inertia rather than viscosity, so the degree of deformation may be deduced from the Weber number. In the current work, intermediate bubbles have Weber numbers larger than unity but less than the critical value at which single bubbles collapse. Therefore, the focus of our study is the flow field around deformed bubbles that have a range of Weber numbers. As Moriguchi and Kato [20] reported, the intermediate bubbles actually cause a certain drag reduction that is insensitive to the bubble size within a range. The drag-reduction mechanism for the range was explained by measuring the componential turbulent shear stress [21]. For high Reynolds numbers, Sanders et al. [10] discussed, using the measured skin

* Corresponding author. Tel./fax: +81 11 706 6373.
E-mail address: oishi@eng.hokudai.ac.jp (Y. Oishi).

http://dx.doi.org/10.1016/j.expthermflusci.2014.02.022
0894-1777/

friction, how drag reduction caused by intermediate bubbles is limited by formation of a liquid layer on the wall. The transition from the microbubble method to the air-film method was investigated by Elbing et al. [22]. Interestingly, they concluded that neither drag-reducing mechanism is persistent in the downstream region owing to the bubble size changing to intermediate size. Hence, the persistence of drag reduction is strongly affected by the intermediate bubbles. In summary, the flow field that is present around intermediate bubbles should be invoked when discussing the persistency of drag reduction.

In our previous study, we measured the variation in local skin friction due to the passage of individual bubbles [23]. A sample of the wall shear stress fluctuation obtained by a shear transducer is shown in Fig. 1. The findings of the previous study were as follows. (1) Individual bubbles considerably reduced the local wall shear stress during their passage. (2) The stress gradually decreased from the front to the rear of the bubble regardless of the bubble size. (3) Stretched bubbles larger than 5 times the boundary layer thickness had zero-skin friction at the rear edge. (4) Wall shear stress increased and oscillated significantly immediately after the passage of each bubble. In this paper, we elucidate such characteristics with the precise measurement of the flow structure around a single bubble suspended in turbulent flow. To start the discussion, the complex relationship of the actual phenomenon should be classified into several stages as illustrated in Fig. 2. Four stages of the interaction between a single bubble and the surrounding shear flow are considered even though the bubble is spherical. The stages are the bubble in uniform flow (Reynolds number problem), the bubble in linear shear flow, the bubble in parabolic shear flow (or linear change in the shear rate), and turbulent shear flow accompanying turbulent shear stress. The same stages must be considered for a deformed bubble as shown in the bottom row of the figure. In linear-shear flow, the deformation of the bubble is characterized by the viscous shear stress, or, capillary number. The parameter is replaced with the Weber number for inertia-dominant turbulent shear flow. The interaction modes in the laminar regime can be numerically analyzed with the Navier–Stokes equation. In contrast, the two-way interaction of the deformed bubble with wall turbulence at high Reynolds number is quite difficult to analytically predict because a full two-way analysis must be carried out treating the free-surface turbulence as well as resolving the liquid flow inside the thin liquid film clinging to the wall. In this context, we apply particle tracking velocimetry (PTV) to a turbulent channel flow in which a single bubble is released in the upstream region. The main control parameter is the Weber number, which expresses the deformability of bubbles in the inertia-dominant boundary layer.

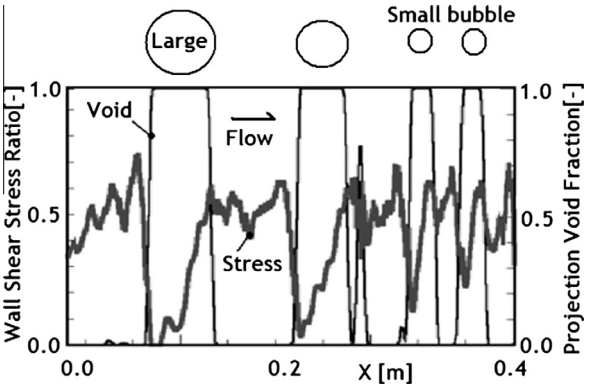

Fig. 1. Fluctuation of local wall shear stress during the passage of bubbles [23].

2. Experimental method

2.1. Test facility

A schematic diagram of the experimental facility is shown in Fig. 3. The test section is a horizontal rectangular channel made of transparent acrylic resin. It is 100 mm width, 10 mm height, and 6000 mm length. Water and air are used as liquid and gas phases at laboratory temperature. Water circulates through the tank, pump, flowmeter, diverging–converging channel, and the test horizontal channel, which includes a bubble injector in its upstream section. The pump is controlled by a frequency that adjusts the flow rate. A schematic diagram of the bubble-injection device is shown in Fig. 4. The device releases a single bubble of pressured air via a regulator. The diameter of the nozzle opening is 13 mm, so as to stably produce a single bubble. The injector is located 250 mm ($L/h = 50$) downstream from the inlet of the horizontal rectangular channel. Filtered water is used; the water is not purified or distilled because small solid tracer particles are eventually seeded to implement PTV. In the case of a small bubble, the water should be considered as contaminated water. However, the contamination does not severely affect the measurement results in the present parametric study because of the high Weber number we are targeting. In the case of a very large bubble injected, the bottom interface of the bubble may protrude beyond the channel central plane. Such a situation strays from the original purpose of our study, but it is also considered as the case that the bubble is wider than the macroscopic shear layer.

Detailed experimental conditions are summarized in Table 1. The mean flow-speed of liquid in the cross section is $U = 1.0$ m/s, which corresponds to $Re = 1 \times 10^4$ (here Re is defined as $Re = 2Uh/\nu$, where h is half the height of the channel and ν is the kinematic viscosity of the liquid). In the table, d is the equivalent bubble diameter observed from the side. The other two Reynolds numbers can be defined to characterize the flow pattern around a single bubble as

$$Re_b = \frac{(U_b - U)d}{\nu}, \quad Re_S = \frac{d}{\nu}\left(\frac{U}{h}d\right) = \frac{d^2U}{\nu h} = \frac{d}{2h}\cdot Re, \tag{1}$$

where U_b stands for the mean bubble velocity. Re_b expresses the flow induced by the streamwise slip velocity. The slip velocity is small in comparison with the velocity difference between the top and bottom of bubbles (see Fig. 2). Thus, the shear Reynolds number, Re_s, relates to the flow, and is simply the multiplication of d/h and the original Reynolds number as described in Eq. (1). While the Reynolds number deals with flow around a bubble, the Weber number characterizes the deformation of the bubble. There are also two types of expressions involved in the Weber number; one defined by flow speed and one by the shear rate as defined in Eq. (2).

$$We = \frac{\rho U_b^2 d}{\sigma}, \quad We_S = \frac{\rho d}{\sigma}\left(\frac{U_b}{h}d\right)^2 = \frac{\rho d^2 U_b^2}{\sigma h} = \frac{d}{h}\cdot We. \tag{2}$$

We employ the former definition, We, in this paper. Using this definition, bubbles begin to prominently deform at Weber numbers larger than 50. Note that Weber number higher than 100 generally implies that the surface tension is irrelevant to the dynamics of the bubble. However, this interpretation is invalid for the present configuration because the bubble in the shear flow maintains its shape with the help of surface tension as long as the bubble has a steady shape. Moreover, the bubble shape in an equilibrium state sensitively depends on the Weber number and it can thus be described by the Weber number.